
Quadrature-based features for kernel approximation

Marina Munkhoeva¹ Yermek Kapushev¹ Evgeny Burnaev¹ Ivan Oseledets¹

Abstract

We consider the problem of improving kernel approximation via randomized feature maps. These maps arise as Monte Carlo approximation to integral representations of kernel functions and scale up kernel methods for larger datasets. We propose to use more efficient numerical integration technique to obtain better estimates of the integrals compared to the state-of-the-art methods. Our approach allows the use of information about the integrand to enhance approximation and facilitates fast computations. We derive the convergence behavior and conduct an extensive empirical study that supports our hypothesis.

1. Introduction

Kernel methods proved to be an efficient technique in numerous real-world problems. The core idea of kernel methods is the kernel trick – compute an inner product in a high-dimensional (or even infinite-dimensional) feature space by means of a kernel function k :

$$k(\mathbf{x}, \mathbf{y}) = \langle \psi(\mathbf{x}), \psi(\mathbf{y}) \rangle, \quad (1)$$

where $\psi : \mathcal{X} \rightarrow \mathcal{F}$ is a non-linear feature map transporting elements of input space \mathcal{X} into a feature space \mathcal{F} . It is a common knowledge that kernel methods incur space and time complexity infeasible to be used with large-scale datasets directly. For example, kernel regression has $\mathcal{O}(N^3 + Nd^2)$ training time, $\mathcal{O}(N^2)$ memory, $\mathcal{O}(Nd)$ prediction time complexity for N data points in original d -dimensional space \mathcal{X} . One of the most successful techniques to handle this problem, known as Random Fourier Features (RFF) (Rahimi & Recht, 2008), introduces a low-dimensional randomized approximation to feature maps:

$$k(\mathbf{x}, \mathbf{y}) \approx \hat{\Psi}(\mathbf{x})^\top \hat{\Psi}(\mathbf{y}). \quad (2)$$

This is essentially carried out by using Monte-Carlo sampling to approximate scalar product in (1). A randomized D -dimensional mapping $\hat{\Psi}(\cdot)$ applied to the original data input allows employing standard linear methods, i.e. reverting the kernel trick. In doing so one reduces the complexity to that of linear methods, e.g. D -dimensional approximation admits $\mathcal{O}(ND^2)$ training time, $\mathcal{O}(ND)$ memory and $\mathcal{O}(N)$ prediction time.

It is well known that as $D \rightarrow \infty$, the inner product in (2) converges to the exact kernel $k(\mathbf{x}, \mathbf{y})$. Recent research (Yang et al., 2014; Felix et al., 2016; Choromanski & Sindhvani, 2016) aims to improve the convergence of approximation so that a smaller D can be used to obtain the same quality of approximation.

This paper considers kernels that allow the following integral representation

$$k(\mathbf{x}, \mathbf{y}) = \mathbb{E}_{p(\mathbf{w})} f_{\mathbf{x}\mathbf{y}}(\mathbf{w}) = I(f_{\mathbf{x}\mathbf{y}}), \quad (3)$$

where $p(\mathbf{w}) = \frac{1}{(2\pi)^{d/2}} e^{-\frac{\|\mathbf{w}\|^2}{2}}$. For example, the popular Gaussian kernel admits such representation, so we can approximate the kernel when $f_{\mathbf{x}\mathbf{y}}(\mathbf{w}) = \phi(\mathbf{w}^\top \mathbf{x})^\top \phi(\mathbf{w}^\top \mathbf{y})$, where $\phi(\cdot) = [\cos(\cdot), \sin(\cdot)]^\top$.

The class of kernels admitting the form in (3) covers shift-invariant kernels (e.g. radial basis function (RBF) kernels) and Pointwise Nonlinear Gaussian (PNG) kernels. They are widely used in practice and have interesting connections with neural networks (Cho & Saul, 2009; Williams, 1997).

The main challenge for the construction of low-dimensional feature maps is the approximation of the expectation in (3) which is d -dimensional integral with Gaussian weight. While standard Monte-Carlo rule is easy to implement, there are better quadrature rules for such kind of integrals. For example, (Yang et al., 2014) apply quasi-Monte Carlo (QMC) rules and obtain better quality kernel matrix approximations compared to random Fourier features of (Rahimi & Recht, 2008).

Unlike other research studies we refrain from using simple Monte Carlo estimate of the integral, instead, we propose to use specific quadrature rules. We now list our contributions:

- We propose to use spherical-radial quadrature rules

¹ Skolkovo Institute of Science and Technology. Correspondence to: Marina Munkhoeva <marina.munkhoeva@skolkovotech.ru>.

to improve kernel approximation accuracy. We also provide an analytical estimate of the error for the used quadrature rules that implies better approximation quality.

- We note that for kernels with specific integrand $f_{\mathbf{xy}}(\mathbf{w})$ in (3) one can improve on its properties. For example, for kernels with even function $f_{\mathbf{xy}}(\mathbf{w})$ we derive the reduced quadrature rule which gives twice smaller embedded dimension D with the same accuracy. This applies, for example, to any RBF kernel.
- We use structured orthogonal matrices (so-called *butterfly matrices*) when designing quadrature rule that allow fast matrix by vector multiplications. As a result, we speed up the approximation of the kernel function and reduce memory requirements.
- We carry out an extensive empirical study comparing our methods with the state-of-the-art ones on a set of different kernels in terms of both kernel approximation error and downstream tasks performance. The study supports our hypothesis on the exceeding accuracy of the method.

2. Quadrature-based random features

We start with rewriting the expectation in equation (3) as integral of $f_{\mathbf{xy}}$ with respect to $p(\mathbf{w})$:

$$I(f_{\mathbf{xy}}) = (2\pi)^{-\frac{d}{2}} \int_{-\infty}^{\infty} \dots \int_{-\infty}^{\infty} e^{-\frac{\mathbf{w}^T \mathbf{w}}{2}} f_{\mathbf{xy}}(\mathbf{w}) d\mathbf{w}.$$

Integration can be performed by means of quadrature rules. The rules usually take a form of interpolating function that is easy to integrate. Given such a rule, one may sample points from the domain of integration and calculate the value of the rule at these points. Then, the sample average of the rule values would yield the approximation of the integral.

The connection between integral approximation and mapping ψ is straightforward. In what follows we show a brief derivation of the quadrature rules that allow for an explicit mapping of the form:

$$\psi(\mathbf{x}) = [a_0 \phi(0) \quad a \phi(\mathbf{w}_1^T \mathbf{x}) \quad \dots \quad a \phi(\mathbf{w}_D^T \mathbf{x})],$$

where the choice of the weights a_0, a and points \mathbf{w}_i is dictated by the quadrature.

We use the average of sampled quadrature rules developed by (Genz & Monahan, 1998) to yield unbiased estimates of $I(f_{\mathbf{xy}})$. A change of coordinates is the first step to facilitate stochastic spherical-radial rules. Now, let $\mathbf{w} = r\mathbf{z}$, with $\mathbf{z}^T \mathbf{z} = 1$, so that $\mathbf{w}^T \mathbf{w} = r^2$ for $r \in [0, \infty]$, leaving us

with (to ease the notation we substitute $f_{\mathbf{xy}}$ with f)

$$I(f) = (2\pi)^{-\frac{d}{2}} \int_{U_d} \int_0^{\infty} e^{-\frac{r^2}{2}} r^{d-1} f(r\mathbf{z}) dr d\mathbf{z} = \frac{(2\pi)^{-\frac{d}{2}}}{2} \int_{U_d} \int_{-\infty}^{\infty} e^{-\frac{r^2}{2}} |r|^{d-1} f(r\mathbf{z}) dr d\mathbf{z}, \quad (4)$$

where $U_d = \{\mathbf{z} : \mathbf{z}^T \mathbf{z} = 1, \mathbf{z} \in \mathbb{R}^d\}$. We are going to use a combination of radial R and spherical S rules of degree three. It has been shown that higher degree rules, being more computationally expensive, often bring in only marginal improvement in performance (Genz & Monahan, 1999). For these reasons in our experiments we use the rule of degree three $SR^{3,3}$, i.e. a combination of radial rule R^3 and spherical rule S^3 . We now describe the logic behind the used quadratures.

Stochastic radial rules. Stochastic radial rule $R(h)$ of degree $2l + 1$ has the form of weighted symmetric sums:

$$R(h) = \sum_{i=0}^l w_i \frac{h(\rho_i) + h(-\rho_i)}{2},$$

which approximates infinite range integral $T(h) = \int_{-\infty}^{\infty} e^{-\frac{r^2}{2}} |r|^{d-1} h(r) dr$. To get an unbiased estimate for $T(h)$, points ρ_i are sampled from specific distributions which depend on the degree of the rule. Weights w_i are derived so that R has a polynomial degree $2l + 1$, i.e. is exact for integrands $h(r) = r^p$ with $p = 0, 1, \dots, 2l + 1$. For radial rules of degree three R^3 the point $\rho_0 = 0$, while $\rho_1 \sim \chi(d + 2)$ follows χ -distribution with $d + 2$ degrees of freedom. Higher degrees require samples from more complex distributions which are hard to sample from.

Stochastic spherical rules. Spherical rule $S(s)$ approximates an integral of a function $s(\mathbf{z})$ over the surface of unit d -sphere U_d and takes the following form:

$$S(s) = \sum_{j=1}^p \tilde{w}_j s(\mathbf{z}_j),$$

where \mathbf{z}_j are points on U_d , i.e. $\mathbf{z}^T \mathbf{z} = 1$. If we set weight $\tilde{w}_j = \frac{|U_d|}{2(d+1)}$ and sum function s values at original and reflected vertices \mathbf{v}_j of randomly rotated d -simplex \mathbf{V} , we will end up with a degree three rule:

$$S_{\mathbf{Q}}^3(s) = \frac{|U_d|}{2(d+1)} \sum_{j=1}^{d+1} [s(-\mathbf{Q}\mathbf{v}_j) + s(\mathbf{Q}\mathbf{v}_j)],$$

where \mathbf{v}_j is the j 'th vertex of d -simplex \mathbf{V} with vertices on U_d and \mathbf{Q} is a random $d \times d$ orthogonal matrix.

Since the value of the integral is approximated as the sample average, the key to unbiased estimate is a proper randomization. In this case, randomization is attained through the matrix \mathbf{Q} . It is crucial to generate uniformly random orthogonal matrices to achieve an unbiased estimate for spherical surface integrals. We consider various designs of such matrices further in Section 3.

Stochastic spherical-radial rules. Meanwhile, combining foregoing rules results in stochastic spherical-radial (*SR*) rule of degree three, in which we plug the integrand f :

$$SR_{\mathbf{Q},\rho}^{3,3}(f) = \left(1 - \frac{d}{\rho^2}\right) f(\mathbf{0}) + \frac{d}{d+1} \sum_{j=1}^{d+1} \left[\frac{f(-\rho\mathbf{Q}\mathbf{v}_j) + f(\rho\mathbf{Q}\mathbf{v}_j)}{2\rho^2} \right], \quad (5)$$

which we finally apply to the approximation of (4) by averaging the samples of $SR_{\mathbf{Q},\rho}^{3,3}$:

$$I(f) = \mathbb{E}_{\mathbf{Q},\rho}[SR_{\mathbf{Q},\rho}^{3,3}(f)] \approx \hat{I}(f) = \frac{1}{n} \sum_{i=1}^n SR_{\mathbf{Q}_i,\rho_i}^{3,3}(f), \quad (6)$$

where n is the number of sampled *SR* rules. Speaking in terms of approximate feature maps, the new feature dimension D in case of quadrature based approximation equals $2n(d+1)$ as we sample n rules and evaluate each of them at $2(d+1)$ points. Surprisingly, empirical results (see Section 5) show that even a small number of rule samples n provides accurate approximations.

In this work we propose to modify the quadrature rule by generating $\rho_j \sim \chi(d+2)$ for each \mathbf{v}_j , i.e.

$$SR_{\mathbf{Q},\rho}^{3,3}(f) = \left(1 - \sum_{j=1}^{d+1} \frac{d}{(d+1)\rho_j^2}\right) f(\mathbf{0}) + \frac{d}{d+1} \sum_{j=1}^{d+1} \left[\frac{f(-\rho_j\mathbf{Q}\mathbf{v}_j) + f(\rho_j\mathbf{Q}\mathbf{v}_j)}{2\rho_j^2} \right].$$

In this case the summands become independent and it reduces the variance of the estimate (it can be seen from the proof of proposition 2.2 which is given in Supplementary Materials).

Explicit mapping. The final form of the mapping is

$$\psi(\mathbf{x}) = [a_0\phi(0) \quad a_1\phi(\mathbf{w}_1^\top\mathbf{x}) \quad \dots \quad a_D\phi(\mathbf{w}_D^\top\mathbf{x})],$$

where $a_0 = \sqrt{1 - \sum_{d=1}^{j=1} \frac{d}{\rho^2}}$, $a_j = \frac{1}{\rho_j} \sqrt{\frac{d}{2(d+1)}}$, \mathbf{w}_j is the row in matrix \mathbf{W} . The matrix $\mathbf{W} = \boldsymbol{\rho} \otimes \begin{bmatrix} (\mathbf{Q}\mathbf{V})^\top \\ -(\mathbf{Q}\mathbf{V})^\top \end{bmatrix}$, where $\boldsymbol{\rho} = [\rho_1 \dots \rho_D]^\top$. To get D features one simply stacks $n = \frac{D}{2(d+1)+1}$ such matrices $\mathbf{W}^k = \boldsymbol{\rho}^k \begin{bmatrix} (\mathbf{Q}^k\mathbf{V})^\top \\ -(\mathbf{Q}^k\mathbf{V})^\top \end{bmatrix}$ so that $\mathbf{W} \in \mathbb{R}^{D \times d}$, where only $\mathbf{Q}^k \in \mathbb{R}^{d \times d}$ and $\boldsymbol{\rho}^k$ ($k = 1, \dots, n$) are generated randomly.

For example, in case of the Gaussian kernel the mapping can be rewritten as ²

$$\psi_G(\mathbf{x}) = [a_0 \quad a_1 \cos(\mathbf{w}_1^\top\mathbf{x}) \quad \dots \quad a_D \cos(\mathbf{w}_D^\top\mathbf{x}) \\ a_1 \sin(\mathbf{w}_1^\top\mathbf{x}) \quad \dots \quad a_D \sin(\mathbf{w}_D^\top\mathbf{x})].$$

Properties of the integrand. We also note here that for specific functions $f_{\mathbf{xy}}(\mathbf{w})$ we can derive better versions of *SR* rule by taking on advantage of the knowledge about the integrand. For example, the Gaussian kernel has $f_{\mathbf{xy}}(\mathbf{w}) = \cos(\mathbf{w}^\top(\mathbf{x} - \mathbf{y}))$. Note that f is even, so we can discard an excessive term in the summation in (2), since $f(\mathbf{w}) = f(-\mathbf{w})$, i.e. *SR*^{3,3} rule reduces to

$$SR_{\mathbf{Q},\rho}^{3,3}(f) = \left(1 - \sum_{j=1}^{d+1} \frac{d}{(d+1)\rho_j^2}\right) f(\mathbf{0}) + \frac{d}{d+1} \sum_{j=1}^{d+1} \frac{f(\rho_j\mathbf{Q}\mathbf{v}_j)}{\rho_j^2}. \quad (7)$$

Variance of the error. We contribute the variance estimation for the stochastic spherical-radial rules when applied to kernel function. To the best of our knowledge, it has not been done before. In case of kernel functions the integrand $f_{\mathbf{xy}}$ can be represented as

$$f_{\mathbf{xy}}(\mathbf{w}) = \phi(\mathbf{w}^\top\mathbf{x})^\top \phi(\mathbf{w}^\top\mathbf{y}) = g(z_1, z_2), \quad (8) \\ z_1 = \mathbf{w}^\top\mathbf{x}, \quad z_2 = \mathbf{w}^\top\mathbf{y},$$

where z_1, z_2 are scalar values. Using this representation of kernel function and its Taylor expansion we can obtain the following proposition (see Supplementary Materials for detailed derivation of the result):

Proposition 2.1. The quadrature rule (6) is an unbiased estimate of integral of any integrable function f . If function f can be represented in the form (8), i.e. $f(\mathbf{w}) = g(z_1, z_2)$, $z_1 = \mathbf{w}^\top\mathbf{x}$, $z_2 = \mathbf{w}^\top\mathbf{y}$ for some $\mathbf{x}, \mathbf{y} \in \mathbb{R}^d$, all 4-th order

¹To get $a_0^2 \geq 0$, you need to sample ρ_j two times on average (see Supplementary Materials for details).

²We do not use reflected points for Gaussian kernel as the integrand f is even, so $\mathbf{W}^k = \frac{\rho^k}{\sigma} (\mathbf{Q}^k\mathbf{V})^\top$.

partial derivatives of g are bounded and $D = 2n(d+1)$ is the number of generated features, then

$$\mathbb{V}[\hat{I}(f)] \leq \frac{0.66M_1^2 l^8 d}{n(d+1)(d+2)} + \frac{53M_1 M_2 l^6}{nd(d+1)(d+2)} + \frac{6M_2^2 l^4}{n(d+1)(d^2-4)}.$$

$$M_1 = \max \left\{ \sup_z \left| \frac{\partial^4 g}{\partial z_1^4} \right|, \sup_z \left| \frac{\partial^4 g}{\partial z_2^4} \right|, \sup_z \left| \frac{\partial^4 g}{\partial z_1^2 \partial z_2^2} \right| \right\},$$

$$M_2 = \max_{j=0,1,2} \left\{ \left| \frac{\partial^2 g}{\partial z_1^j \partial z_2^{2-j}}(0,0) \right| \right\}, \quad l \text{ is a radius of compact set } \mathcal{X}.$$

Proposition 2.2. Let $|\phi(\mathbf{w}^\top \mathbf{x})| \leq \kappa$ for all $\mathbf{w} \in \mathbb{R}^d$ and $\mathbf{x} \in \mathcal{X}$. Then for any $\mathbf{x}, \mathbf{y} \in \mathcal{X}$ it holds

$$\mathbb{V}(\hat{I}(f)) \leq \frac{2 + \kappa^4 + \kappa^2}{n(d-2)}$$

This proposition is simpler but applies only for bounded $\phi(\cdot)$ functions.

To give rationale on why our method works we can consider the error bound on $\|\hat{I}(f) - k\|_\infty$. In (Sutherland & Schneider, 2015) the probability $\mathbb{P}(\|\hat{I}(f) - k\|_\infty \geq \epsilon)$ was estimated for RFF. Following the same proof strategy for our quadrature rules as in (Sutherland & Schneider, 2015), but using Chebyshev-Cantelli inequality instead of Hoeffding's and Bernstein inequalities (as they are not applicable in this case) we can obtain the following result (see details in Supplementary Materials).

Let us compare which method gives higher error at the same probability level, i.e. find errors $\epsilon_I, \epsilon_{RFF}$ such that

$$\mathbb{P}(\|\hat{k}_{RFF} - k\|_\infty \geq \epsilon_{RFF}) = \mathbb{P}(\|\hat{I}(f) - k\|_\infty \geq \epsilon_I).$$

When $\phi(\cdot) = [\cos(\cdot), \sin(\cdot)]$, $\kappa = 1$, solving the above equation for $\epsilon_I, \epsilon_{RFF}$, we obtain

$$\epsilon_I^2 = \left(\frac{\epsilon_{RFF}^2}{\sigma_I^2 \sigma_{RFF}^2} + \frac{4}{D \sigma_I^2} \right) \left(\frac{2d}{3(d+1)} \right)^d - \frac{4\sigma_I^2}{D},$$

where σ_{RFF} and σ_I are variance estimates in RFF and $\hat{I}(f)$ expressions, respectively. We can see the term $\frac{2d}{3(d+1)} < 1$, thus, for large dimensions d it is easy to see that $\epsilon_I < \epsilon_{RFF}$, i.e. our method has lower error at the same probability level. For another typical case with small input dimensions d and large number of samples D : $\epsilon_I^2 \approx \frac{\epsilon_{RFF}^2}{\sigma_I^2 \sigma_{RFF}^2} \left(\frac{2d}{3(d+1)} \right)^d$, so the error of the proposed method is less when $\frac{1}{\sigma_I^2 \sigma_{RFF}^2} \left(\frac{2d}{3(d+1)} \right)^d < 1$. For RBF kernel $\sigma_{RFF}^2 \geq \frac{1}{2}$, $\sigma_I^2 > \frac{4(d+1)}{d-2}$ and for our method the error is less when $\frac{d-2}{2(d+1)} \left(\frac{2d}{3(d+1)} \right)^d < 1$ which is always the case.

However, we have used rather crude Chebyshev-Cantelli inequality. It can be refined using more accurate upper bound but it needs some technical work which is postponed for the future work.

The quadrature rule (2) grants us some freedom in the choice of random orthogonal matrix \mathbf{Q} . The next section discusses such matrices and suggests *butterfly matrices* for fast matrix by vector multiplication as the *SR* rule implementation involves multiplication of the matrix $\mathbf{Q}\mathbf{V}$ by the data vector.

3. Generating uniformly random orthogonal matrices

Previously described stochastic spherical-radial rules require a random orthogonal matrix \mathbf{Q} (see equation (2)). If \mathbf{Q} follows Haar distribution on the set of all matrices in the orthogonal group $O(d)$ in dimension d , then the averages of spherical rules $S_{\mathbf{Q}_i}^3(s)$ provide unbiased degree three estimates for integrals over unit sphere. Essentially, Haar distribution means that all orthogonal matrices in the group are equiprobable, i.e. uniformly random. Methods for sampling such matrices vary in their complexity of generation and multiplication.

Techniques based on QR decomposition (Mezzadri, 2006) have complexity cubic in d , and the resulting matrix does not allow fast matrix by vector multiplications. Another set of methods is based on a sequence of reflectors ((Stewart, 1980)) or rotators (Anderson et al., 1987). The complexity is better (quadratic in d), however the resulting matrix is unstructured and, thus, implicates no fast matrix by vector multiplication. In (Choromanski et al., 2017) random orthogonal matrices are considered. They are constructed as a product of random diagonal matrices and Hadamard matrices and therefore enable fast matrix by vector products. Unfortunately, they are not guaranteed to follow the Haar distribution.

To satisfy both our requirements, i.e. low computational/space complexity and generation of Haar distributed orthogonal matrices, we propose to use so-called *butterfly matrices*.

Butterfly matrices. The method from (Genz, 1998) generates Haar distributed random orthogonal matrix \mathbf{B} . As it happens to be a product of butterfly structured factors, a matrix of this type conveniently possesses the property of fast multiplication. For $d = 4$ an example of butterfly orthogonal matrix is

$$\mathbf{B}^{(4)} = \begin{bmatrix} c_1 & -s_1 & 0 & 0 \\ s_1 & c_1 & 0 & 0 \\ 0 & 0 & c_3 & -s_3 \\ 0 & 0 & s_3 & c_3 \end{bmatrix} \begin{bmatrix} c_2 & 0 & -s_2 & 0 \\ 0 & c_2 & 0 & -s_2 \\ s_2 & 0 & c_2 & 0 \\ 0 & s_2 & 0 & c_2 \end{bmatrix} = \begin{bmatrix} c_1 c_2 & -s_1 c_2 & -c_1 s_2 & s_1 s_2 \\ s_1 c_2 & c_1 c_2 & -s_1 s_2 & -c_1 s_2 \\ c_3 s_2 & -s_3 s_2 & c_3 c_2 & -s_3 c_2 \\ s_3 s_2 & c_3 s_2 & s_3 c_2 & c_3 c_2 \end{bmatrix}.$$

Definition 3.1. Let $c_i = \cos \theta_i$, $s_i = \sin \theta_i$ for $i = 1, \dots, d-1$ be given. Assume $d = 2^k$ with $k > 0$. Then

an orthogonal matrix $\mathbf{B}^{(d)} \in \mathbb{R}^{d \times d}$ is defined recursively as follows

$$\mathbf{B}^{(2d)} = \begin{bmatrix} \mathbf{B}^{(d)} c_d & -\mathbf{B}^{(d)} s_d \\ \hat{\mathbf{B}}^{(d)} s_d & \hat{\mathbf{B}}^{(d)} c_d \end{bmatrix}, \quad \mathbf{B}^{(1)} = 1,$$

where $\hat{\mathbf{B}}^{(d)}$ is the same as $\mathbf{B}^{(d)}$ with indexes i shifted by d , e.g.

$$\mathbf{B}^{(2)} = \begin{bmatrix} c_1 & -s_1 \\ s_1 & c_1 \end{bmatrix}, \quad \hat{\mathbf{B}}^{(2)} = \begin{bmatrix} c_3 & -s_3 \\ s_3 & c_3 \end{bmatrix}.$$

Matrix $\mathbf{B}^{(d)}$ by vector product has computational complexity $O(d \log d)$ since $\mathbf{B}^{(d)}$ has $\lceil \log d \rceil$ factors and each factor requires $O(d)$ operations. Another advantage is space complexity: $\mathbf{B}^{(d)}$ is fully determined by $d - 1$ angles θ_i , yielding $O(d)$ memory complexity.

The randomization is based on the sampling of angles θ . The key to uniformly random orthogonal butterfly matrix \mathbf{B} is the sequence of $d - 1$ angles θ_i . To get $\mathbf{B}^{(d)}$ Haar distributed, we follow (Fang & Li, 1997) algorithm that first computes a uniform random point \mathbf{u} from U_d . It then calculates the angles by taking the ratios of the appropriate \mathbf{u} coordinates $\theta_i = \frac{u_i}{u_{i+1}}$, followed by computing cosines and sines of the θ 's.

One can easily define butterfly matrix $\mathbf{B}^{(d)}$ for the cases when d is not a power of two (see Supplementary Materials for details). The method that uses butterfly orthogonal matrices is denoted by \mathbf{B} in the experiments section.

4. Kernels

This section gives examples on how quadrature rules can be applied to a number of kernels.

4.1. Gaussian kernel

Radial basis function (RBF) kernels are popular kernels widely used in kernel methods. Gaussian kernel is a widely exploited RBF kernel and has the following form:

$$k(\mathbf{x}, \mathbf{y}) = \exp\left(-\frac{\|\mathbf{x} - \mathbf{y}\|^2}{2\sigma^2}\right).$$

In this case the integral representation has $\phi(\mathbf{w}^\top \mathbf{x}) = [\cos(\mathbf{w}^\top \mathbf{x}), \sin(\mathbf{w}^\top \mathbf{x})]^\top$. Since $f_{\mathbf{x}\mathbf{y}}(0) = 1$, $SR^{3,3}$ rule for Gaussian kernel has the form (σ appears due to scaling):

$$SR_{\mathbf{Q}, \rho}^{3,3}(f) = 1 - \sum_{j=1}^{d+1} \frac{d}{(d+1)\rho_j^2} + \frac{d}{d+1} \sum_{j=1}^{d+1} \frac{f\left(\frac{\rho_j \mathbf{Q}\mathbf{v}_j}{\sigma}\right)}{\rho_j^2},$$

4.2. Arc-cosine kernels

Arc-cosine kernels were originally introduced by (Cho & Saul, 2009) upon studying the connections between deep

Table 1. Space and time complexity for different kernel approximation algorithms.

Method	Space	Time
ORF	$\mathcal{O}(Dd)$	$\mathcal{O}(Dd)$
QMC	$\mathcal{O}(Dd)$	$\mathcal{O}(Dd)$
ROM	$\mathcal{O}(d)$	$\mathcal{O}(d \log d)$
Quadrature based	$\mathcal{O}(d)$	$\mathcal{O}(d \log d)$

learning and kernel methods. The integral representation of the b^{th} -order arc-cosine kernel is

$$k_b(\mathbf{x}, \mathbf{y}) = 2 \int_{\mathbb{R}^d} \phi_b(\mathbf{w}^\top \mathbf{x}) \phi_b(\mathbf{w}^\top \mathbf{y}) p(\mathbf{w}) d\mathbf{w},$$

where $\phi_b(\mathbf{w}^\top \mathbf{x}) = \Theta(\mathbf{w}^\top \mathbf{x})(\mathbf{w}^\top \mathbf{x})^b$, $\Theta(\cdot)$ is the Heaviside function and p is the density of the standard Gaussian distribution. Such kernels can be seen as an inner product between the representation produced by infinitely wide single layer neural network with random Gaussian weights. They have closed form expressions in terms of the angle $\theta = \cos^{-1}\left(\frac{\mathbf{x}^\top \mathbf{y}}{\|\mathbf{x}\| \|\mathbf{y}\|}\right)$ between \mathbf{x} and \mathbf{y} .

The 0-order arc-cosine kernel is given by $k_0(\mathbf{x}, \mathbf{y}) = 1 - \frac{\theta}{\pi}$, the 1-order kernel is given by $k_1(\mathbf{x}, \mathbf{y}) = \frac{\|\mathbf{x}\| \|\mathbf{y}\|}{\pi} (\sin \theta + (\pi - \theta) \cos \theta)$.

Let $\phi_0(\mathbf{w}^\top \mathbf{x}) = \Theta(\mathbf{w}^\top \mathbf{x})$ and $\phi_1(\mathbf{w}^\top \mathbf{x}) = \max(0, \mathbf{w}^\top \mathbf{x})$, then we can rewrite the integral representation as follows: $k_b(\mathbf{x}, \mathbf{y}) = 2 \int_{\mathbb{R}^d} \phi_b(\mathbf{w}^\top \mathbf{x}) \phi_b(\mathbf{w}^\top \mathbf{y}) p(\mathbf{w}) d\mathbf{w} \approx \frac{2}{n} \sum_{i=1}^n SR_{\mathbf{Q}_i, \rho_i}^{3,3}$. For arc-cosine kernel of order 0 the value of the function $\phi_0(0) = \Theta(0) = 0.5$ results in

$$SR_{\mathbf{Q}, \rho}^{3,3}(f) = 0.25 \left(1 - \sum_{j=1}^{d+1} \frac{d}{(d+1)\rho_j^2} \right) + \frac{d}{d+1} \sum_{j=1}^{d+1} \frac{f(\rho_j \mathbf{Q}\mathbf{v}_j) + f(-\rho_j \mathbf{Q}\mathbf{v}_j)}{2\rho_j^2}.$$

In the case of arc-cosine kernel of order 1, the value of $\phi_1(0)$ is 0 and the $SR^{3,3}$ rule reduces to

$$SR_{\mathbf{Q}, \rho}^{3,3}(f) = \frac{d}{d+1} \sum_{j=1}^{d+1} \frac{f(|\rho \mathbf{Q}\mathbf{v}_j|)}{2\rho_j^2}.$$

5. Experiments

We extensively study the proposed method on several established benchmarking datasets: Powerplant, LETTER, USPS, MNIST, CIFAR100 (Krizhevsky & Hinton, 2009), LEUKEMIA (Golub et al., 1999). In Section 5.2 we show kernel approximation error across different kernels and

number of features. We also report the quality of SVM models with approximate kernels on the same data sets in Section 5.3. The compared methods are described below.

5.1. Methods

We present a comparison of our method with estimators based on a simple Monte Carlo, quasi-Monte Carlo (Yang et al., 2014) and Gaussian quadratures (Dao et al., 2017). The Monte Carlo approach has a variety of ways to generate samples: unstructured Gaussian (Rahimi & Recht, 2008), structured Gaussian (Felix et al., 2016), random orthogonal matrices (ROM) (Choromanski et al., 2017).

Monte Carlo integration (G, Gort, ROM). The kernel is estimated as $\hat{k}(\mathbf{x}, \mathbf{y}) = \frac{1}{D} \phi(\mathbf{M}\mathbf{x})\phi(\mathbf{M}\mathbf{y})$, where $\mathbf{M} \in \mathbb{R}^{D \times d}$ is a random weight matrix. For unstructured Gaussian based approximation $\mathbf{M} = \mathbf{G}$, where $\mathbf{G}_{ij} \sim \mathcal{N}(0, 1)$. Structured Gaussian has $\mathbf{M} = \mathbf{G}_{\text{ort}}$, where $\mathbf{G}_{\text{ort}} = \mathbf{D}\mathbf{Q}$, \mathbf{Q} is obtained from RQ decomposition of \mathbf{G} , \mathbf{D} is a diagonal matrix with diagonal elements sampled from the $\chi(d)$ distribution. In compliance with the previous work on ROM we use S-Rademacher with three blocks: $\mathbf{M} = \sqrt{d} \prod_{i=1}^3 \mathbf{S}\mathbf{D}_i$ since three blocks have been shown to yield the best results.

Quasi-Monte Carlo integration (QMC). Quasi-Monte Carlo integration boasts improved rate of convergence $1/D$ compared to $1/\sqrt{D}$ of Monte Carlo, however, empirical results illustrate its performance is poorer than that of orthogonal random features (Felix et al., 2016). It has larger constant factor hidden under \mathcal{O} notation in computational complexity. For QMC the weight matrix \mathbf{M} is generated as a transformation of quasi-random sequences. We run our experiments with Halton sequences in compliance with the previous work.

Gaussian quadratures (GQ). We included subsampled dense grid method from (Dao et al., 2017) into our comparison as it is the only data-independent approach from the paper that is shown to work well. We reimplemented code for the paper to the best of our knowledge as it is not open sourced.

Quadrature rules (B). Our main method that uses stochastic spherical-radial rules with $\mathbf{Q} = \tilde{\mathbf{B}}$ (butterfly matrix)³ is denoted by **B**.

5.2. Kernel approximation

To measure kernel approximation quality we use relative error in Frobenius norm $\frac{\|\mathbf{K} - \hat{\mathbf{K}}\|_F}{\|\mathbf{K}\|_F}$, where \mathbf{K} and $\hat{\mathbf{K}}$ denote exact kernel matrix and its approximation. In line

³ $\tilde{\mathbf{B}} = (\mathbf{B}\mathbf{P})_1(\mathbf{B}\mathbf{P})_2 \dots (\mathbf{B}\mathbf{P})_3$, where \mathbf{P} is a permutation matrix, for explanation see Supplementary Materials.

with previous work we run experiments for the kernel approximation on a random subset of a dataset. Table 2 displays the settings for the experiments across the datasets.

Table 2. Experimental settings for the datasets. N is the total number of objects, d is dimensionality of the original feature space. The number of samples and runs used in experiments is denoted as # samples, # runs, respectively.

Dataset	N	d	# samples	# runs
Powerplant	9568	4	550	500
LETTER	20000	16	550	500
USPS	9298	256	550	500
MNIST	70000	784	550	100
CIFAR100	60000	3072	50	50
LEUKEMIA	72	7129	10	10

Approximation was constructed for different number of SR samples $n = \frac{D}{2(d+1)+1}$, where d is an original feature space dimensionality and D is the new one. For the Gaussian kernel we set hyperparameter $\gamma = \frac{1}{2\sigma^2}$ to the default value of $\frac{1}{d}$ for all the approximants, while arc-cosine kernels have no hyperparameters.

We run experiments for each [kernel, dataset, n] tuple and plot 95% confidence interval around the mean value line. Figure 1 shows the results for kernel approximation error on LETTER, MNIST, CIFAR100 and LEUKEMIA datasets.

QMC method almost always coincides with RFF except for arc-cosine 0 kernel. It particularly enjoys Powerplant dataset with $d = 4$, i.e. small number of features. Possible explanation for such behaviour can be due to the connection with QMC quadratures. The worst case error for QMC quadratures scales with $n^{-1}(\log n)^d$, where d is the dimensionality and n is the number of sample points (Owen, 1998). It is worth mentioning that for large d it is also a problem to construct a proper QMC point set. Thus, in higher dimensions QMC may bring little practical advantage over MC. GQ method as well matches the performance of RFF. We omit both QMC and GQ from experiments on datasets with large $d = [3072, 7129]$ (CIFAR100, LEUKEMIA).

We also omitted method **H** as it coincides with the proposed **B** everywhere, which is expected as the **B** method is only different from **H** in the choice of the matrix \mathbf{Q} to facilitate speed up. Figure 1 demonstrates the empirical results which support our hypothesis about the advantages of SR quadratures applied to kernel approximation compared to SOTA methods. Although, for the Gaussian kernel, **B** does almost coincide with ROM and Gort, except for the one case (Powerplant, arc-cosine 0 kernel), our method displays exceeding performance.

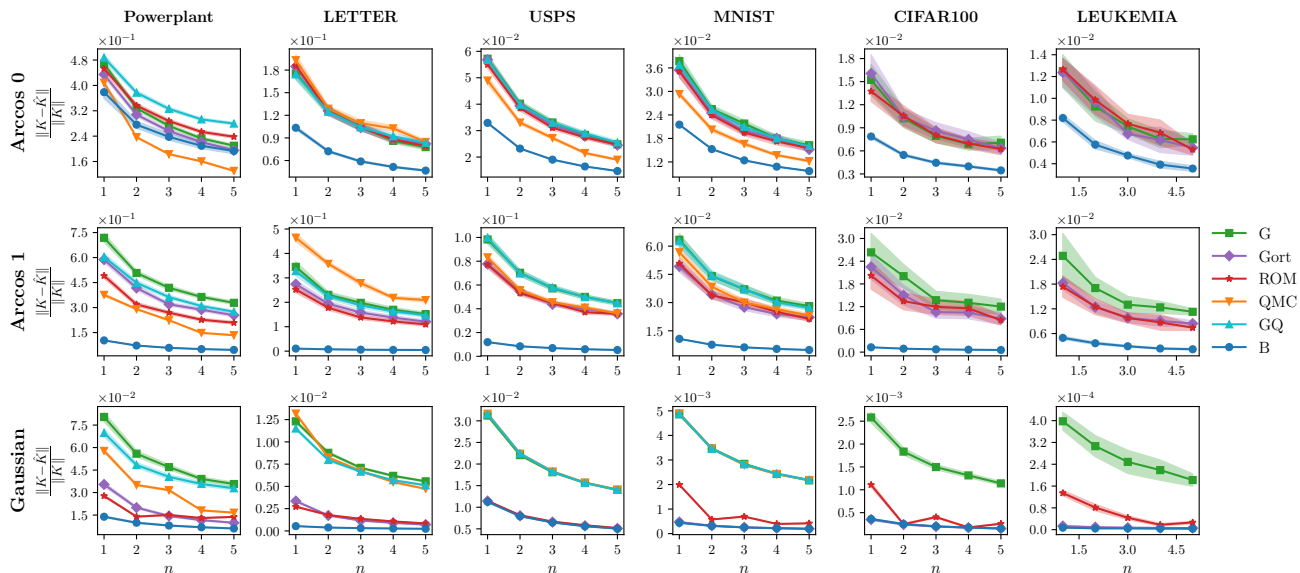


Figure 1. Kernel approximation error across three kernels and 6 datasets. Lower is better. The x-axis represents the factor to which we extend the original feature space, $n = \frac{D}{2(d+1)+1}$, where d is the dimensionality of the original feature space, D is the dimensionality of the new feature space.

5.3. Classification/regression with new features

We report accuracy and R^2 scores for the classification/regression tasks on some of the datasets (Figure 2). We examine the performance with the same setting as in experiments for kernel approximation error, except now we map the whole dataset. We use Support Vector Machines to obtain predictions.

Kernel approximation error does not fully define the final prediction accuracy – the best performing kernel matrix approximant not necessarily yields the best accuracy or R^2 score. However, the empirical results illustrate that our method delivers comparable and often superior quality on the downstream tasks.

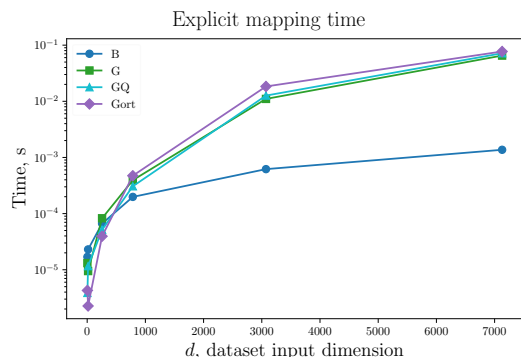


Figure 3. Time spent on explicit mapping. The x-axis represents the 5 datasets with increasing input number of features: LETTER, Powerplant, USPS, MNIST, CIFAR100 and LEUKEMIA.

5.4. Walltime experiment

We measure time spent on explicit mapping of features. Indeed, Figure 3 demonstrates that the method scales as theoretically predicted with larger dimensions thanks to the structured nature of the mapping.

6. Related work

The most popular methods for scaling up kernel methods are based on a low-rank approximation of the kernel using either data-dependent or independent basis functions. The first one includes Nyström method (Drineas & Mahoney, 2005), greedy basis selection techniques (Smola & Schölkopf, 2000), incomplete Cholesky decomposition (Fine & Scheinberg, 2001).

The construction of basis functions in these techniques utilizes the given training set making them more attractive for some problems compared to Random Fourier Features approach. In general, data-dependent approaches perform better than data-independent approaches when there is a gap in the eigen-spectrum of the kernel matrix. The rigorous study of generalization performance of both approaches can be found in (Yang et al., 2012).

In data-independent techniques, the kernel function is approximated directly. Most of the methods (including the proposed approach) that follow this idea are based on Random Fourier Features (Rahimi & Recht, 2008). They require so-called weight matrix that can be generated in a

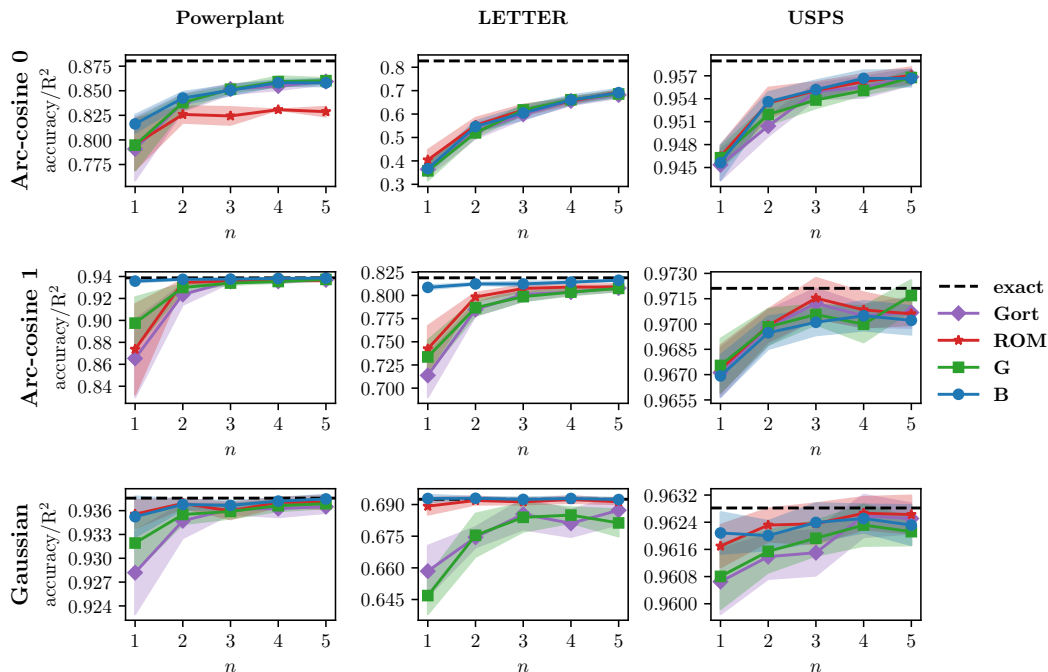


Figure 2. Accuracy/ R^2 score using embeddings with three kernels on 3 datasets. Higher is better. The x-axis represents the factor to which we extend the original feature space, $n = \frac{D}{2(d+1)+1}$.

number of ways. (Le et al., 2013) form the weight matrix as a product of structured matrices. It enables fast computation of matrix-vector products and speeds up generation of random features.

Another work (Felix et al., 2016) orthogonalizes the features by means of orthogonal weight matrix. This leads to less correlated and more informative features increasing the quality of approximation. They support this result both analytically and empirically. The authors also introduce matrices with some special structure for fast computations. (Choromanski et al., 2017) propose a generalization of the ideas from (Le et al., 2013) and (Felix et al., 2016), delivering an analytical estimate for the mean squared error (MSE) of approximation.

All these works use simple Monte Carlo sampling. However, the convergence can be improved by changing Monte Carlo sampling to Quasi-Monte Carlo sampling. Following this idea (Yang et al., 2014) apply quasi-Monte Carlo to Random Fourier Features. In (Yu et al., 2015) the authors make attempt to improve quality of the approximation of Random Fourier Features by optimizing sequences conditioning on a given dataset.

Among the recent papers there are works that, similar to our approach, use the numerical integration methods to approximate kernels. While (Bach, 2017) carefully inspects the connection between random features and quadratures, they did not provide any practically useful explicit mappings

for kernels. Leveraging the connection (Dao et al., 2017) propose several methods with Gaussian quadratures. Among them three schemes are data-independent and one is data-dependent. The authors do not compare them with the approaches for random feature generation other than random Fourier features. The data-dependent scheme optimizes the weights for the quadrature points to yield better performance.

7. Conclusion

In this work we proposed to apply advanced integration rule that allowed us to achieve higher quality of kernel approximation. To speed up the computations we employed butterfly orthogonal matrices yielding the computational complexity $\mathcal{O}(d \log d)$.

Our experimental study confirms that for many kernels on the most datasets the proposed approach delivers the best kernel approximation. Additionally, the results showed that the quality of the downstream task (classification/regression) is also superior or comparable to the state-of-the-art baselines. The connection between the downstream score and the kernel approximation error is left as future work.

References

Anderson, Theodore W, Olkin, Ingram, and Underhill, Les G. Generation of random orthogonal matrices. *SIAM*

- Journal on Scientific and Statistical Computing*, 8(4): 625–629, 1987.
- Bach, Francis. On the equivalence between kernel quadrature rules and random feature expansions. *Journal of Machine Learning Research*, 18(21):1–38, 2017.
- Cho, Youngmin and Saul, Lawrence K. Kernel methods for deep learning. In *Advances in Neural Information Processing Systems*, pp. 342–350, 2009.
- Choromanski, Krzysztof and Sindhvani, Vikas. Recycling randomness with structure for sublinear time kernel expansions. *arXiv preprint arXiv:1605.09049*, 2016.
- Choromanski, Krzysztof, Rowland, Mark, and Weller, Adrian. The unreasonable effectiveness of random orthogonal embeddings. *arXiv preprint arXiv:1703.00864*, 2017.
- Dao, Tri, De Sa, Christopher M, and Ré, Christopher. Gaussian quadrature for kernel features. In *Advances in Neural Information Processing Systems*, pp. 6109–6119, 2017.
- Drineas, Petros and Mahoney, Michael W. On the Nyström method for approximating a Gram matrix for improved kernel-based learning. *Journal of Machine Learning Research*, 6(Dec):2153–2175, 2005.
- Fang, Kai-Tai and Li, Run-Ze. Some methods for generating both an NT-net and the uniform distribution on a Stiefel manifold and their applications. *Computational Statistics & Data Analysis*, 24(1):29–46, 1997.
- Felix, X Yu, Suresh, Ananda Theertha, Choromanski, Krzysztof M, Holtmann-Rice, Daniel N, and Kumar, Sanjiv. Orthogonal Random Features. In *Advances in Neural Information Processing Systems*, pp. 1975–1983, 2016.
- Fine, Shai and Scheinberg, Katya. Efficient SVM training using low-rank kernel representations. *Journal of Machine Learning Research*, 2(Dec):243–264, 2001.
- Genz, Alan. Methods for generating random orthogonal matrices. *Monte Carlo and Quasi-Monte Carlo Methods*, pp. 199–213, 1998.
- Genz, Alan and Monahan, John. Stochastic integration rules for infinite regions. *SIAM journal on scientific computing*, 19(2):426–439, 1998.
- Genz, Alan and Monahan, John. A stochastic algorithm for high-dimensional integrals over unbounded regions with gaussian weight. *Journal of Computational and Applied Mathematics*, 112(1):71–81, 1999.
- Golub, Todd R, Slonim, Donna K, Tamayo, Pablo, Huard, Christine, Gaasenbeek, Michelle, Mesirov, Jill P, Coller, Hilary, Loh, Mignon L, Downing, James R, Caligiuri, Mark A, et al. Molecular classification of cancer: class discovery and class prediction by gene expression monitoring. *Science*, 286(5439):531–537, 1999.
- Krizhevsky, Alex and Hinton, Geoffrey. Learning multiple layers of features from tiny images. 2009.
- Le, Quoc, Sarlós, Tamás, and Smola, Alex. Fastfood-approximating kernel expansions in loglinear time. In *Proceedings of the International Conference on Machine Learning*, 2013.
- Mezzadri, Francesco. How to generate random matrices from the classical compact groups. *arXiv preprint math-ph/0609050*, 2006.
- Owen, Art B. Latin supercube sampling for very high-dimensional simulations. *ACM Transactions on Modeling and Computer Simulation (TOMACS)*, 8(1): 71–102, 1998.
- Rahimi, Ali and Recht, Benjamin. Random features for large-scale kernel machines. In *Advances in Neural Information Processing Systems*, pp. 1177–1184, 2008.
- Smola, Alex J and Schölkopf, Bernhard. Sparse greedy matrix approximation for machine learning. 2000.
- Stewart, G. W. The efficient generation of random orthogonal matrices with an application to condition estimators. *SIAM Journal on Numerical Analysis*, 17(3):403–409, 1980. ISSN 00361429. URL <http://www.jstor.org/stable/2156882>.
- Sutherland, Dougal J and Schneider, Jeff. On the error of random fourier features. *arXiv preprint arXiv:1506.02785*, 2015.
- Williams, Christopher KI. Computing with infinite networks. In *Advances in Neural Information Processing Systems*, pp. 295–301, 1997.
- Yang, Jiyan, Sindhvani, Vikas, Avron, Haim, and Mahoney, Michael. Quasi-Monte Carlo feature maps for shift-invariant kernels. In *Proceedings of The 31st International Conference on Machine Learning (ICML-14)*, pp. 485–493, 2014.
- Yang, Tianbao, Li, Yu-Feng, Mahdavi, Mehrdad, Jin, Rong, and Zhou, Zhi-Hua. Nyström Method vs Random Fourier Features: A Theoretical and Empirical Comparison. In *Advances in Neural Information Processing Systems*, pp. 476–484, 2012.
- Yu, Felix X, Kumar, Sanjiv, Rowley, Henry, and Chang, Shih-Fu. Compact nonlinear maps and circulant extensions. *arXiv preprint arXiv:1503.03893*, 2015.

Quadrature-based features for kernel approximation. Supplementary materials.

8. Obtaining a proper ρ

It may be the case when sampling ρ that $1 - \sum_{j=1}^{d+1} \frac{d}{(d+1)\rho_j^2} < 0$ which results in complex a_0 term. Simple solution is just to resample ρ_j to satisfy the non-negativity of the expression. According to central limit theorem $\sum_{j=1}^{d+1} \frac{d}{(d+1)\rho_j^2}$ tends to normal random variable with mean 1 and variance $\frac{1}{d+1} \frac{2}{d-2}$. The probability that this values is non-negative equals $p = \mathbb{P}(1 - \sum_{j=1}^{d+1} \frac{d}{(d+1)\rho_j^2} \geq 0) \rightsquigarrow \frac{1}{2}$. The expectation of number of resamples needed to satisfy non-negativity constraint is $\frac{1}{p}$ tends to 2.

9. Butterfly matrices generation details

9.1. Not a power of two

We discuss here the procedure to generate butterfly matrices of size $d \times d$ when d is not a power of 2.

Let the number of butterfly factors $k = \lceil \log d \rceil$. Then $\mathbf{B}^{(d)}$ is constructed as a product of k factor matrices of size $d \times d$ obtained from k matrices used for generating $\mathbf{B}^{(2^k)}$. For each matrix in the product for $\mathbf{B}^{(2^k)}$, we delete the last $2^k - d$ rows and columns. We then replace with 1 every c_i in the remaining $d \times d$ matrix that is in the same column as deleted s_i .

For the cases when d is not a power of two, the resulting \mathbf{B} has deficient columns with zeros (Figure 4(b), right), which introduces a bias to the integral estimate. To correct for this bias one may apply additional randomization by using a product $\mathbf{B}\mathbf{P}$, where $\mathbf{P} \in \{0, 1\}^{d \times d}$ is a permutation matrix. Even better, use a product of several $\mathbf{B}\mathbf{P}$'s: $\tilde{\mathbf{B}} = (\mathbf{B}\mathbf{P})_1(\mathbf{B}\mathbf{P})_2 \dots (\mathbf{B}\mathbf{P})_t$. We set $t = 3$ in the experiments.

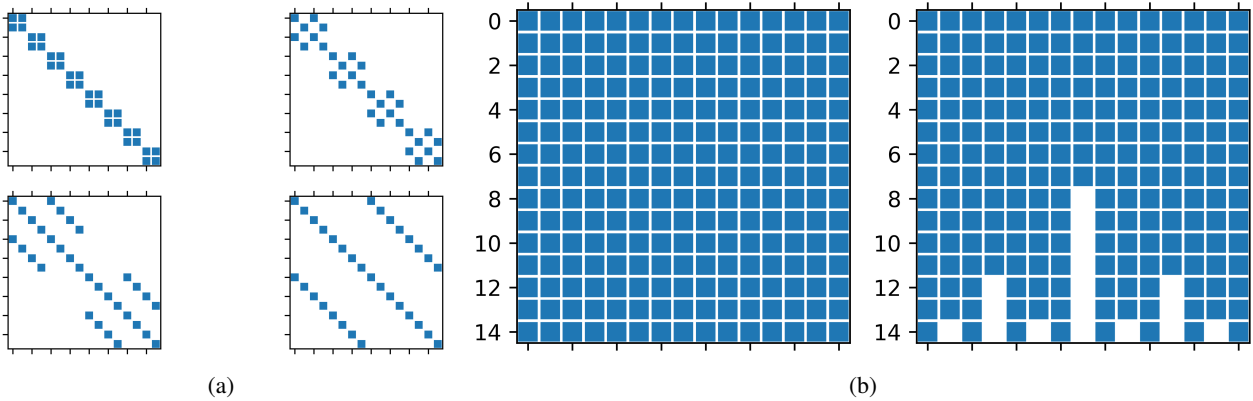


Figure 4. (a) Butterfly orthogonal matrix factors for $d = 16$. (b) Sparsity pattern for $\mathbf{B}\mathbf{P}\mathbf{B}\mathbf{P}\mathbf{B}\mathbf{P}$ (left) and \mathbf{B} (right), $d = 15$.

10. Variance of kernel function approximation using quadrature rule

The function $f_{\mathbf{x}\mathbf{y}}$ in quadrature rule can be considered as a function of two variables, i.e. $f_{\mathbf{x}\mathbf{y}} = \phi(\mathbf{w}^\top \mathbf{x})\phi(\mathbf{w}^\top \mathbf{y}) = g(z_1, z_2)$, where $z_1 = \mathbf{w}^\top \mathbf{x}$, $z_2 = \mathbf{w}^\top \mathbf{y}$.

In the quadrature rule $\rho \sim \chi(d+2)$ and \mathbf{Q} is a random orthogonal matrix. Therefore, random variables $\mathbf{w}_i = \mathbf{Q}\mathbf{v}_i$ are uniformly distributed on a unit-sphere.

Now, let's write down 4-th order Taylor expansion with Lagrange remainder of the function $g(\rho_i \mathbf{w}_i^\top \mathbf{x}, \rho_i \mathbf{w}_i^\top \mathbf{y}) + g(-\rho_i \mathbf{w}_i^\top \mathbf{x}, -\rho_i \mathbf{w}_i^\top \mathbf{y})$ around 0 (odd terms cancel out)

$$g(\rho_i \mathbf{w}_i^\top \mathbf{x}, \rho_i \mathbf{w}_i^\top \mathbf{y}) + g(-\rho_i \mathbf{w}_i^\top \mathbf{x}, -\rho_i \mathbf{w}_i^\top \mathbf{y}) \approx 2g(0, 0) + 2 \sum_{j=0}^2 \frac{c_j}{j!(2-j)!} (\mathbf{w}_i^\top \mathbf{x})^j (\mathbf{w}_i^\top \mathbf{y})^{2-j} + \\ + \rho_i^2 \sum_{j=0}^4 \frac{d_j^i}{j!(4-j)!} (\mathbf{w}_i^\top \mathbf{x})^j (\mathbf{w}_i^\top \mathbf{y})^{4-j}$$

where $c_j = \frac{\partial^2 g}{\partial z_1^j \partial z_2^{2-j}}(0, 0)$, $d_j^i = \frac{\partial^4 g}{\partial z_1^j \partial z_2^{4-j}}(\epsilon_1^i, \epsilon_2^i) + \frac{\partial^4 g}{\partial z_1^j \partial z_2^{4-j}}(\epsilon_3^i, \epsilon_4^i)$, ϵ_1^i is between 0 and $(\rho_i \mathbf{w}_i^\top \mathbf{x})$, ϵ_2^i is between 0 and $(\rho_i \mathbf{w}_i^\top \mathbf{y})$, ϵ_3^i is between 0 and $(-\rho_i \mathbf{w}_i^\top \mathbf{x})$ and ϵ_4^i is between 0 and $(-\rho_i \mathbf{w}_i^\top \mathbf{y})$.

Plugging this expression into quadrature rule we obtain

$$SR_{\mathbf{Q}, \rho}^{3,3}(f_{\mathbf{x}\mathbf{y}}) \approx \left(1 - \frac{1}{d+1} \sum_{i=1}^{d+1} \frac{d}{\rho_i^2}\right) g(0, 0) + \\ + \sum_{i=1}^{d+1} \left[\frac{dg(0, 0)}{(d+1)\rho_i^2} + \frac{d}{(d+1)\rho_i^2} \sum_{j=0}^2 \frac{c_j}{j!(2-j)!} (\mathbf{w}_i^\top \mathbf{x})^j (\mathbf{w}_i^\top \mathbf{y})^{2-j} + \right. \\ \left. \frac{d}{2(d+1)} \sum_{j=0}^4 \frac{d_j}{j!(4-j)!} (\mathbf{w}_i^\top \mathbf{x})^j (\mathbf{w}_i^\top \mathbf{y})^{4-j} \right] = \\ = g(0, 0) + \frac{d}{d+1} \sum_{i=1}^{d+1} S_i,$$

where $S_i = A_i + B_i$, $A_i = \frac{1}{\rho_i^2} \sum_{j=0}^2 \frac{c_j}{j!(2-j)!} (\mathbf{w}_i^\top \mathbf{x})^j (\mathbf{w}_i^\top \mathbf{y})^{2-j}$, $B_i = \frac{1}{2} \sum_{j=0}^4 \frac{d_j^i}{j!(4-j)!} (\mathbf{w}_i^\top \mathbf{x})^j (\mathbf{w}_i^\top \mathbf{y})^{4-j}$, $\mathbf{w}_j = \mathbf{Q}\mathbf{v}_j$, matrix \mathbf{Q} is a random orthogonal matrix uniformly distributed on a set of orthogonal matrices $O(n)$. From uniformity of orthogonal matrix \mathbf{Q} it follows that vector \mathbf{w}_j is uniform on a unit n -sphere. Also note that S_i and S_j are independent if $i \neq j$, therefore, $Cov(S_i, S_j) = 0$.

Let us calculate the variance of the estimate.

$$\mathbb{V} \left[SR_{\mathbf{Q}, \rho}^{3,3}(f_{\mathbf{x}\mathbf{y}}) \right] = \frac{d^2}{(d+1)^2} \mathbb{V} \left[\sum_{j=1}^{d+1} S_j \right] = \frac{d^2}{(d+1)^2} \sum_{i=1}^{d+1} \mathbb{V}(S_i) = \frac{d^2}{(d+1)} \mathbb{V}(S_1) \quad (9)$$

Distribution of random variable ρ is $\chi(d+2)$, therefore

$$\mathbb{E} \left(\frac{1}{\rho^2} \right) = \frac{1}{d}, \quad \mathbb{E} \left(\frac{1}{\rho^4} \right) = \frac{1}{d(d-2)}, \quad d > 2.$$

Now, let us calculate the variance $\mathbb{V}S_i$ from the first term of equation (9)

$$\mathbb{V}S_i = \mathbb{V}(A_i + B_i) = \mathbb{V}(A_i) + \mathbb{V}(B_i) + Cov(A_i, B_i).$$

Let $\|\mathbf{x}\| \geq \|\mathbf{y}\|$. Then

$$\begin{aligned}
 \mathbb{V}(B_i) &= \frac{1}{4} \mathbb{V} \left(\sum_{j=0}^4 \frac{d_j^i (\mathbf{w}_i^\top \mathbf{x})^j (\mathbf{w}_i^\top \mathbf{y})^{4-j}}{j!(4-j)!} \right) \leq \frac{1}{4} \mathbb{E} \left(\sum_{j=0}^4 \frac{d_j^i (\mathbf{w}_i^\top \mathbf{x})^j (\mathbf{w}_i^\top \mathbf{y})^{4-j}}{j!(4-j)!} \right)^2 = \\
 &= \frac{1}{4} \mathbb{E} \left(\frac{(d_0^i)^2 (\mathbf{w}^\top \mathbf{y})^8 + (d_4^i)^2 (\mathbf{w}^\top \mathbf{x})^8}{596} + \frac{(4(d_1^i)^2 + 3d_0^i d_2^i) (\mathbf{w}^\top \mathbf{x})^2 (\mathbf{w}^\top \mathbf{y})^6}{144} + \right. \\
 &\quad \left. \frac{(4(d_3^i)^2 + 3d_4^i d_2^i) (\mathbf{w}^\top \mathbf{x})^6 (\mathbf{w}^\top \mathbf{y})^2}{144} + \right. \\
 &\quad \left. \frac{(1296(d_2^i)^2 + 72d_0^i d_4^i + 1152d_1^i d_3^i) (\mathbf{w}^\top \mathbf{x})^4 (\mathbf{w}^\top \mathbf{y})^4}{20736} \right) \leq \\
 &\leq \frac{M_1^2}{1192} \mathbb{E} (\mathbf{w}^\top \mathbf{x})^8 + \frac{7M_1^2}{296} \|\mathbf{x}\|^2 \mathbb{E} (\mathbf{w}^\top \mathbf{x})^6 + 0.031M_1^2 \|\mathbf{x}\|^4 \mathbb{E} (\mathbf{w}^\top \mathbf{x})^4, \tag{10}
 \end{aligned}$$

where $M_1 = \max \left\{ \sup_z \left| \frac{\partial^4 g}{\partial z_1^4} (z_1, z_2) \right|, \sup_z \left| \frac{\partial^4 g}{\partial z_2^4} (z_1, z_2) \right|, \sup_z \left| \frac{\partial^4 g}{\partial z_1^2 \partial z_2^2} (z_1, z_2) \right| \right\}$.

To calculate expectations of the form $\mathbb{E}(\mathbf{w}^\top \mathbf{x})^k$ we will use expression for integral of monomial over unit sphere (?)

$$J(k_1, k_2, \dots, k_d) = \int_{S_{d-1}} \mathbf{x}_1^{k_1} \mathbf{x}_2^{k_2} \dots \mathbf{x}_d^{k_d} d\mathbf{x} = \sigma_d \frac{(k_1 - 1)!! (k_2 - 1)!! \dots (k_d - 1)!!}{d(d+2) \dots (d+|k|-2)}, \tag{11}$$

where $k_i = 2s_i, s_i \in \mathbb{Z}_+, |k| = \sum_i k_i, \sigma_d$ is a volume of an d -dimensional unit sphere.

For example, let us show how to calculate $\mathbb{E}(\mathbf{w}^\top \mathbf{x})^4$:

$$\begin{aligned}
 \mathbb{E}(\mathbf{w}^\top \mathbf{x})^4 &= \mathbb{E} \sum_{i,j,k,m} \mathbf{w}_i \mathbf{w}_j \mathbf{w}_k \mathbf{w}_m \mathbf{x}_i \mathbf{x}_j \mathbf{x}_k \mathbf{x}_m = \\
 &= \left[\text{thanks to symmetry all terms, for which at least one index doesn't coincide with} \right. \\
 &\quad \left. \text{other indices, are equal to 0.} \right] = \mathbb{E} \left[\sum_i \mathbf{w}_i^4 \mathbf{x}_i^4 + 3 \sum_{i \neq j} \mathbf{w}_i^2 \mathbf{w}_j^2 \mathbf{x}_i^2 \mathbf{x}_j^2 \right] = \\
 &= \frac{3}{d(d+2)} \sum_i \mathbf{x}_i^4 + \frac{3}{d(d+2)} \sum_{i \neq j} \mathbf{x}_i^2 \mathbf{x}_j^2 = \frac{3}{d(d+2)} \|\mathbf{x}\|^4.
 \end{aligned}$$

Using the same technique for (10) we obtain

$$\begin{aligned}
 \mathbb{V}(B_i) &\leq \frac{1}{4} M_1^2 \|\mathbf{x}\|^8 \left(\frac{8.46}{d(d+2)(d+4)(d+6)} + \frac{10.21}{d(d+2)(d+4)} + \frac{0.37}{d(d+2)} \right) \leq \\
 &\leq \frac{0.67M_1^2 \|\mathbf{x}\|^8}{d(d+2)} \tag{12}
 \end{aligned}$$

For the variance of A_i we have

$$\begin{aligned}
 \mathbb{V}(A_i) &= \mathbb{V} \left(\frac{1}{\rho_i^2} \sum_{j=0}^2 \frac{c_j (\mathbf{w}_i^T \mathbf{x})^j (\mathbf{w}_i^T \mathbf{y})^{2-j}}{j!(2-j)!} \right) \leq \mathbb{E} \left(\frac{1}{\rho_i^2} \sum_{j=0}^2 \frac{c_j (\mathbf{w}_i^T \mathbf{x})^j (\mathbf{w}_i^T \mathbf{y})^{2-j}}{j!(2-j)!} \right)^2 = \\
 &= \frac{1}{d(d-2)} \mathbb{E} \left(\sum_{j=0}^2 \frac{c_j (\mathbf{w}_i^T \mathbf{x})^j (\mathbf{w}_i^T \mathbf{y})^{2-j}}{j!(2-j)!} \right)^2 = \\
 &= \frac{1}{d(d-2)} \left(\frac{3c_0^2 \|\mathbf{x}\|^4 + 3c_2^2 \|\mathbf{y}\|^4 + (4c_1^2 + 2c_0c_2)(\|\mathbf{x}\|^2 \|\mathbf{y}\|^2 + 2(\mathbf{x}^T \mathbf{y})^2)}{4d(d+2)} \right) \leq \\
 &\leq \left[\text{we assume that } \|\mathbf{x}\| \geq \|\mathbf{y}\| \right] \leq \frac{6}{d^2(d^2-4)} M_2^2 \|\mathbf{x}\|^4, \tag{13}
 \end{aligned}$$

where $M_2 = \max_{j=0,1,2} \left\{ \left| \frac{\partial^2 g}{\partial z_1^j \partial z_2^{2-j}}(0,0) \right| \right\}$.

Let's estimate covariance $Cov(A_i, B_i)$:

$$Cov(A_i, B_i) \leq \mathbb{E}(A_i B_i) + |\mathbb{E}A_i \mathbb{E}B_i|.$$

The first term of the right hand side:

$$\begin{aligned}
 \mathbb{E} \left(\frac{1}{\rho^2} \sum_{j=0}^2 \frac{c_j (\mathbf{w}_i^T \mathbf{x})^j (\mathbf{w}_i^T \mathbf{y})^{2-j}}{j!(2-j)!} \frac{1}{2} \sum_{j=0}^4 \frac{d_j^i (\mathbf{w}_i^T \mathbf{x})^j (\mathbf{w}_i^T \mathbf{y})^{4-j}}{j!(4-j)!} \right) \leq \\
 \left[\text{we assume that } \|\mathbf{x}\| \geq \|\mathbf{y}\| \right] \leq \frac{53M_1 M_2 \|\mathbf{x}\|^6}{d^2(d+2)(d+4)}.
 \end{aligned}$$

The second term $\mathbb{E}A_i \mathbb{E}B_i$ (again for $\|\mathbf{x}\| \geq \|\mathbf{y}\|$)

$$|\mathbb{E}A_i \mathbb{E}B_i| \leq \frac{M_1 M_2 \|\mathbf{x}\|^6}{2d^3(d+2)}.$$

Combining the derived inequalities we obtain

$$\begin{aligned}
 \mathbb{V}S_i &\leq \frac{6}{d^2(d^2-4)} M_2^2 \|\mathbf{x}\|^4 + \frac{0.67M_1^2 \|\mathbf{x}\|^8}{d(d+2)} + \frac{53M_1 M_2 \|\mathbf{x}\|^6}{d^2(d+2)(d+4)} + \frac{M_1 M_2 \|\mathbf{x}\|^6}{2d^3(d+2)} \leq \\
 &\leq \frac{0.67M_1^2 \|\mathbf{x}\|^8}{d(d+2)} + \frac{53M_1 M_2 \|\mathbf{x}\|^6}{d^3(d+2)} + \frac{6M_2^2 \|\mathbf{x}\|^4}{d^2(d^2-4)}. \tag{14}
 \end{aligned}$$

Substituting (14) into (9) we obtain

$$\begin{aligned}
 \mathbb{V} \left[SR_{\mathbf{Q}, \rho}^{3,3}(f_{\mathbf{xy}}) \right] &\leq \frac{d^2}{d+1} \left(\frac{0.66M_1^2 \|\mathbf{x}\|^8}{d(d+2)} + \frac{53M_1 M_2 \|\mathbf{x}\|^6}{d^3(d+2)} + \frac{6M_2^2 \|\mathbf{x}\|^4}{d^2(d^2-4)} \right) = \\
 &= \frac{0.66M_1^2 \|\mathbf{x}\|^8 d}{(d+1)(d+2)} + \frac{53M_1 M_2 \|\mathbf{x}\|^6}{d(d+1)(d+2)} + \frac{6M_2^2 \|\mathbf{x}\|^4}{(d+1)(d^2-4)}
 \end{aligned}$$

And finally

$$\mathbb{V} \left[\frac{1}{n} \sum_{i=1}^n SR_{\mathbf{Q}_i, \rho_i}^{3,3}(f_{\mathbf{xy}}) \right] \leq \frac{0.66M_1^2 \|\mathbf{x}\|^8 d}{n(d+1)(d+2)} + \frac{53M_1 M_2 \|\mathbf{x}\|^6}{nd(d+1)(d+2)} + \frac{6M_2^2 \|\mathbf{x}\|^4}{n(d+1)(d^2-4)}.$$

11. Proof of Proposition 2.2

Let us denote $\mathbf{q} = \begin{pmatrix} \mathbf{x} \\ \mathbf{y} \end{pmatrix} \in \mathcal{X}^2$, $k(\mathbf{q}) = k(\mathbf{x}, \mathbf{y})$, $h_j(\mathbf{q}) = d \frac{f_{\mathbf{x}\mathbf{y}}(-\rho_j \mathbf{Q}\mathbf{v}_j) + f_{\mathbf{x}\mathbf{y}}(\rho_j \mathbf{Q}\mathbf{v}_j)}{2\rho_j^2} - k(\mathbf{q}) = s_j(\mathbf{q}) - k(\mathbf{q})$. Then it is easy to see that $\mathbb{E}h_j(\mathbf{q}) = 0$.

Let us denote $I(\mathbf{q}) = SR_{\mathbf{Q}_1, \rho_1}^{3,3}(f_{\mathbf{x}\mathbf{y}})$, $g(\mathbf{q}) = I(\mathbf{q}) - k(\mathbf{x}, \mathbf{y})$. Using the above definitions we obtain

$$\mathbb{V}g(\mathbf{q}) = \mathbb{V} \left(1 - \sum_{j=1}^{d+1} \frac{d}{(d+1)\rho_j^2} \right) + \mathbb{E} \left(\frac{1}{d+1} \sum_{i=1}^{d+1} h_i(\mathbf{q}) \right)^2 + 2cov \left(1 - \sum_{j=1}^{d+1} \frac{d}{(d+1)\rho_j^2}, \frac{1}{d+1} \sum_{i=1}^{d+1} h_i(\mathbf{q}) \right). \quad (15)$$

Variance of the first term

$$\begin{aligned} \mathbb{V} \left(1 - \sum_{j=1}^{d+1} \frac{d}{(d+1)\rho_j^2} \right) &= \mathbb{E} \left(1 - \sum_{j=1}^{d+1} \frac{d}{(d+1)\rho_j^2} \right)^2 = \mathbb{E} \left(1 - \sum_{j=1}^{d+1} \frac{2d}{(d+1)\rho_j^2} + \left(\sum_{j=1}^{d+1} \frac{d}{(d+1)\rho_j^2} \right)^2 \right) = \\ &= 1 - 2 + \frac{d}{(d+1)(d-2)} + \frac{d}{d+1} = \frac{2}{(d+1)(d-2)}. \end{aligned} \quad (16)$$

Variance of the second term (using independence of $h_i(\mathbf{q})$ and $h_j(\mathbf{q})$ for $i \neq j$)

$$\mathbb{E} \left(\frac{1}{d+1} \sum_{i=1}^{d+1} h_i(\mathbf{q}) \right)^2 = \mathbb{E} \left(\frac{1}{(d+1)^2} \sum_{i,j=1}^{d+1} h_i(\mathbf{q})h_j(\mathbf{q}) \right) = \frac{1}{(d+1)^2} \sum_{i=1}^{d+1} \mathbb{E}h_i(\mathbf{q})^2 = \frac{\mathbb{E}h_1(\mathbf{q})^2}{d+1}. \quad (17)$$

Variance of the last term (using Cauchy-Schwarz inequality)

$$\begin{aligned} cov \left(1 - \sum_{j=1}^{d+1} \frac{d}{(d+1)\rho_j^2}, \frac{1}{d+1} \sum_{i=1}^{d+1} h_i(\mathbf{q}) \right) &= \mathbb{E} \left[\left(1 - \sum_{j=1}^{d+1} \frac{d}{(d+1)\rho_j^2} \frac{1}{d+1} \right) \sum_{i=1}^{d+1} h_i(\mathbf{q}) \right] = \\ &= -\mathbb{E} \frac{d}{d+1} \sum_{i,j=1}^{d+1} \frac{h_i(\mathbf{q})}{\rho_j^2} \leq \frac{1}{d+1} \sum_{i=1}^{d+1} \sqrt{\mathbb{E} \frac{1}{\rho_i^4}} \sqrt{\mathbb{E}h_i(\mathbf{q})^2} = \sqrt{\frac{\mathbb{E}h_1(\mathbf{q})^2}{d(d-2)}}. \end{aligned} \quad (18)$$

Now, let us upper bound term $\mathbb{E}h_1(\mathbf{q})^2$

$$\mathbb{E}h_1(\mathbf{q})^2 = \mathbb{E} \left(\frac{d\phi(\mathbf{w}^\top \mathbf{x})\phi(\mathbf{w}^\top \mathbf{y})}{\rho^2} \right)^2 - k(\mathbf{q})^2 \leq \frac{d\kappa^4}{d-2}.$$

Using this expression and plugging (16), (17), (18) into (15) we obtain

$$\begin{aligned} \mathbb{V} \left[\frac{1}{n} \sum_{i=1}^n SR_{\mathbf{Q}_i, \rho_i}^{3,3}(f_{\mathbf{x}\mathbf{y}}) \right] &\leq \frac{2}{n(d+1)(d-2)} + \frac{d\kappa^4}{n(d+1)(d-2)} + \frac{1}{n} \sqrt{\frac{d\kappa^4}{d(d-2)^2}} \leq \\ &\leq \frac{2}{n(d+1)(d-2)} + \frac{d\kappa^4}{n(d+1)(d-2)} + \frac{\kappa^2}{n(d-2)} \leq \frac{2 + \kappa^4 + \kappa^2}{n(d-2)}. \end{aligned} \quad (19)$$

and it concludes the proof.

12. Derivation of error probability

The proof strategy closely follows that of (Sutherland & Schneider, 2015); we just use Chebyshev-Cantelli inequality instead of Hoeffding's and Bernstein inequalities and all the expectations are calculated according to our quadrature rules.

Let $\mathbf{q} = \begin{pmatrix} \mathbf{x} \\ \mathbf{y} \end{pmatrix} \in \mathcal{X}^2$, \mathcal{X}^2 is compact set in \mathbb{R}^{2d} with diameter $\sqrt{2}l$, so we can cover it with an ε -net using at most $T = (2\sqrt{2}l/r)^{2d}$ balls of radius r . Let $\{\mathbf{q}_i\}_{i=1}^T$ denote their centers, and L_g be the Lipschitz constant of $g(\mathbf{q}) : \mathbb{R}^{2d} \rightarrow \mathbb{R}$. If $|g(\mathbf{q}_i)| < \varepsilon/2$ for all i and $L_g < \varepsilon/(2r)$, then $g(\mathbf{q}) < \varepsilon$ for all $\mathbf{q} \in \mathcal{X}^2$.

12.1. Regularity Condition

Similarly to (Sutherland & Schneider, 2015) (regularity condition section in appendix) it can be proven that $\mathbb{E}\nabla g(\mathbf{q}) = \nabla\mathbb{E}g(\mathbf{q})$.

12.2. Lipschitz Constant

Since g is differentiable, $L_g = \|\nabla g(\mathbf{q}^*)\|$, where $\mathbf{q}^* = \arg \max_{\mathbf{q} \in \mathcal{X}^2} \|\nabla g(\mathbf{q})\|$. Via Jensen's inequality $\mathbb{E}\|\nabla h(\mathbf{q})\| \geq \|\mathbb{E}\nabla h(\mathbf{q})\|$. Then using independence of $h_i(\mathbf{q})$ and $h_j(\mathbf{q})$ for $i \neq j$

$$\begin{aligned} \mathbb{E}[L_g]^2 &= \mathbb{E} \left[\|\nabla I(\mathbf{q}^*) - k(\mathbf{q}^*)\|^2 \right] = \mathbb{E} \left[\left\| \frac{1}{d+1} \sum_{i=1}^{d+1} \nabla h_i(\mathbf{q}^*) \right\|^2 \right] = \mathbb{E} \left[\frac{1}{d+1} \|\nabla h_1(\mathbf{q}^*)\|^2 \right] = \\ &= \frac{1}{d+1} \mathbb{E}_{\mathbf{q}^*} \left[\mathbb{E} \|\nabla s_1(\mathbf{q}^*)\|^2 - 2\|\nabla k(\mathbf{q}^*)\| \mathbb{E} \|\nabla s_1(\mathbf{q}^*)\| + \|\nabla k(\mathbf{q}^*)\|^2 \right] \leq \\ &\leq \frac{1}{d+1} \mathbb{E} \left[\|\nabla s_1(\mathbf{q}^*)\|^2 - \|\nabla k(\mathbf{q}^*)\|^2 \right] \leq \frac{1}{d+1} \mathbb{E} \|\nabla s_1(\mathbf{q}^*)\|^2 = \\ &= \frac{1}{d+1} \mathbb{E} \left[\|\nabla_{\mathbf{x}^*} s_1(\mathbf{q}^*)\|^2 + \|\nabla_{\mathbf{y}^*} s_1(\mathbf{q}^*)\|^2 \right] \leq \frac{2d^2 \kappa^2 \mu^2 \sigma_p^2}{d+1} \mathbb{E} \frac{1}{\rho_1^2} = \frac{2d\kappa^2 \mu^2 \sigma_p^2}{d+1}, \end{aligned}$$

where $|\phi'(\cdot)| \leq \mu$. Then using Markov's inequality we obtain

$$\mathbb{P}(L_g \geq \frac{\varepsilon}{2r}) \leq 8 \frac{d}{d+1} \left(\frac{\sigma_p r \kappa \mu}{\varepsilon} \right)^2$$

12.3. Anchor points

Let us upper bound the following probability using Chebyshev-Cantelli inequality

$$\mathbb{P} \left(\bigcup_{i=1}^T |g(\mathbf{q}_i)| \geq \frac{1}{2}\varepsilon \right) \leq T \mathbb{P} \left(|g(\mathbf{q}_i)| \geq \frac{1}{2}\varepsilon \right) \leq \frac{\mathbb{V}(g(\mathbf{q}))}{\mathbb{V}(g(\mathbf{q})) + \varepsilon^2/4} = 2 \left(\frac{2\sqrt{2}l}{r} \right)^{2d} \frac{\sigma_I^2}{\sigma_I^2 + D\varepsilon^2/4},$$

where σ_I is such that $\mathbb{V}(g(\mathbf{q})) = \mathbb{V}(I(\mathbf{q})) = \sigma_I^2/D$.

12.4. Optimizing over r

Now the probability of $\sup_{\mathbf{q} \in \mathcal{X}^2} |g(\mathbf{q})| \leq \varepsilon$ takes the form

$$p = \mathbb{P} \left(\sup_{\mathbf{q} \in \mathcal{X}^2} |g(\mathbf{q})| \leq \varepsilon \right) \geq 1 - \kappa_1 r^{-2d} - \kappa_2 r^2,$$

where $\kappa_1 = 2 \left(2\sqrt{2}l \right)^{2d} \frac{\sigma_I^2}{\sigma_I^2 + D\varepsilon^2/4}$, $\kappa_2 = \frac{8d}{d+1} \left(\frac{\kappa \mu \sigma_p}{\varepsilon} \right)^2$. Maximizing this probability over r gives us the following bound

$$\mathbb{P} \left(\sup_{\mathbf{q} \in \mathcal{X}^2} |g(\mathbf{q})| \geq \varepsilon \right) \leq \left(d^{\frac{-d}{d+1}} + d^{\frac{1}{d+1}} \right) 2^{\frac{6d+1}{d+1}} \left(\frac{d}{d+1} \right)^{\frac{d}{d+1}} \left(\frac{\sigma_p l \kappa \mu}{\varepsilon} \right)^{\frac{2d}{d+1}} \left(\frac{\sigma_I^2}{\sigma_I^2 + D\varepsilon^2/4} \right)^{\frac{1}{d+1}}.$$